

RSC Advances

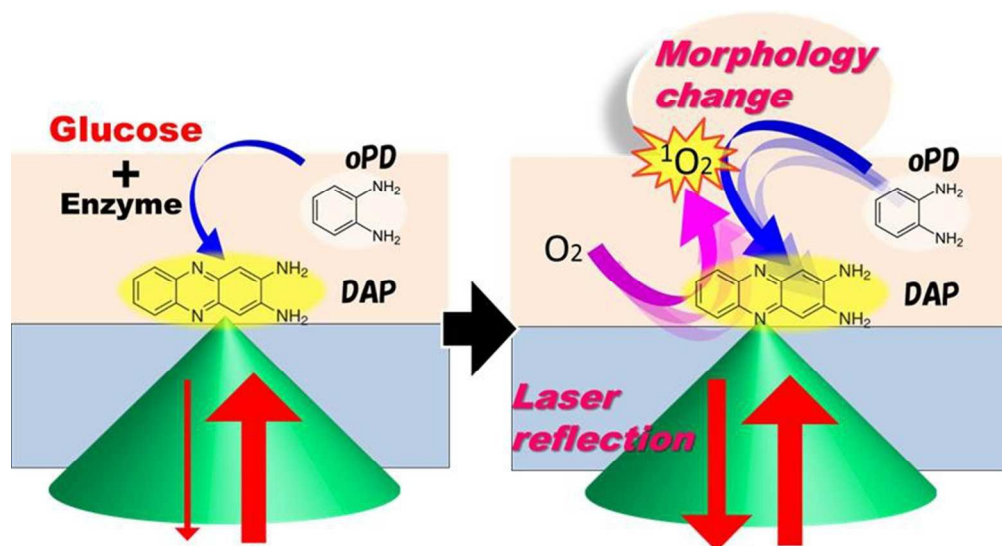


This is an *Accepted Manuscript*, which has been through the Royal Society of Chemistry peer review process and has been accepted for publication.

Accepted Manuscripts are published online shortly after acceptance, before technical editing, formatting and proof reading. Using this free service, authors can make their results available to the community, in citable form, before we publish the edited article. This *Accepted Manuscript* will be replaced by the edited, formatted and paginated article as soon as this is available.

You can find more information about *Accepted Manuscripts* in the [Information for Authors](#).

Please note that technical editing may introduce minor changes to the text and/or graphics, which may alter content. The journal's standard [Terms & Conditions](#) and the [Ethical guidelines](#) still apply. In no event shall the Royal Society of Chemistry be held responsible for any errors or omissions in this *Accepted Manuscript* or any consequences arising from the use of any information it contains.



The mechanism of glucose sensing based on the laser-induced morphology change
72x39mm (300 x 300 DPI)

A new methodology for optical biosensing with drop-casting fabrication of sensor chips and irradiation/detection of a single laser beam

H. Yoshikawa*, S. Imura and E. Tamiya

We propose a new methodology for optical biosensing with drop-casting fabrication of sensor chips and irradiation/detection of a single laser beam. Glucose sensor chips were fabricated by simply depositing a solution, including *o*-phenylenediamine (oPD), glucose oxidase (GOD), and horseradish peroxidase (HRP), on a glass substrate. A sample solution was dropped on the sensor chip and the concentration was detected by measuring the reflection intensity of the laser beam focused on the chip. A surface deformation induced by the laser irradiation on the chip was observed by electron microscopy, demonstrating that this sensor chip converts the enzyme reactions into morphological changes using the assistance of the laser beam. The mechanism of the laser-induced surface deformation was investigated by testing the effect of sodium azide and fluorescence spectroscopy.

Introduction

Various methodologies and platforms have been proposed for biosensor chips. MEMS and nanotechnologies have enabled fabrication of microscale electrodes, QCMs, plasmonic nanostructures on chips to convert biological reactions such as enzymatic reactions, antigen-antibody interactions, and DNA hybridizations to electronic or optical signals¹⁻⁶. Although these approaches increase sensor performance dramatically, they can also greatly increase the cost of biosensor chips. The integration of micro-sensing elements in biosensor chips without expenditure of time, labour, and cost is required for the practical use. One approach using molecular systems, which convert biological reactions to mechanical changes and optical signals, is proposed in this paper. Light-induced surface and morphological deformation of organic materials and its potential applications in optical storage, microactuators, and sensing devices are gaining increasing attention from researchers^{7,8}. The most representative materials are azobenzene and its derivative molecules. The formation of a surface relief grating on an azopolymer film was observed after irradiation of a light with an optical interference pattern^{9,10}. This light-induced deformation was attributed to photoisomerisation and photoinduced anisotropy of azobenzene groups^{11,12}. Irie et al. observed reversible morphology changes of a diarylethene single crystal upon light irradiation¹³. Such light-induced deformation originates from molecular conformational changes induced by photochemical reactions. The mechanisms and dynamics, including excited energy relaxation and

photochemical reaction processes, in addition to the relationship between nano- or micro-scale deformation and molecular-scale conformational changes have been studied^{14, 15}. However, although various applications of these phenomena have been proposed, they have not been established practically. In this paper, we prepared a film composed of *o*-phenylenediamine (oPD) and enzymes, which shows light-induced surface deformation in the presence of substrates of the enzymes. This idea originated from our previous work concerning single-beam optical biosensing¹⁶. oPD, an aniline derivative, forms poly(oPD) as a result of oxidative polymerization. We found that local polymerization was induced by focusing a visible laser beam on the oPD solution, and we succeeded in glucose detection by combining this reaction with enzyme reactions. However, this method requires the mixing of oPD and the enzyme solution in the sample. If these components could be immobilized on a sensor plate, the sensing procedure would be simplified. Immobilization of enzymes is an important research topic in research fields related to biosensors, bioreactors, and bioanalysis¹⁷⁻²⁰. Various methods have been employed for enzyme immobilization, including adsorption, entrapment, and chemical linking to gels, polymers, and membranes. Generally, materials (matrices) to immobilize enzymes are required to have high bio-affinity and hold enzymes without inhibiting enzyme activity. In this study, we prepared a thin film of oPD and enzymes in a simple way and confirmed its bio- and photo-chemical function. The mechanism of the laser-induced deformation was investigated by fluorescence microspectroscopy and by addition of radical

quenchers. The laser-induced surface deformation associated with enzymatic reactions was detected based on the reflected intensity of the focused laser beam, and glucose detection was also demonstrated.

Experimental

Drop-casting fabrication of sensor chips

The fabrication procedure for the sensor chip is schematically illustrated in Figure 1. *o*-phenylenediamine (oPD) obtained from Sigma Aldrich was dissolved in citrate buffer (pH 4.8) at 1 mM. Glucose oxidase (Toyobo Enzyme, >100 U/mg) and horseradish peroxidase (Wako, >100 U/mg) were also dissolved in citrate buffer at 1 and 0.1 mg/mL, respectively. These conditions of sample preparation were almost the same as those of previous experiment¹⁶. Equal amounts of these solutions were mixed together. A silicon rubber sheet (thickness 0.2 mm) with 3-mm holes was placed on a glass plate (Matsunami, 24 × 36 mm, thickness 0.12–0.17 mm). The solution described above (10 μL) was dropped into each hole on the glass plate. Composite films of oPD, GOD and HRP formed in the holes after the water was removed by drying in a vacuum chamber (- 40 kPa) for 90 min at room temperature. The sensor chips were stored in a freezer at -20 °C until use.

Laser irradiation and fluorescence measurement using a microscope

The experimental setup to induce changes in surface morphology and detect the reflected laser intensity is shown in Figure 2. A DPSS green laser beam (Shanghai Dream Lasers, SDL-532-020TL, wavelength: 532 nm) was introduced to an optical inverted microscope (Olympus, IX70) via a beam expander. The laser beam was focused by using an objective lens (60x, N.A. 0.9) on an oPD film. The laser intensity was set at 2 mW at the laser focus. The x-y position of the sample and the laser irradiation time were controlled by a motorized stage and a mechanical shutter, respectively. The reflected light of the green laser beam was detected using a photomultiplier (Hamamatsu Photonics, R1166). The output voltage of the photomultiplier was recorded at a 50 Hz sampling rate by using a data acquisition device (National Instruments, USB-6341). For fluorescence spectrum measurement, a DPSS blue laser beam (Shanghai Dream Lasers, SDL-473-050TL, wavelength: 473 nm) was focused on a sensor plate or 2,3-diaminophenazine (DAP, Sigma Aldrich) powder via the same objective lens and the fluorescence spectrum from the laser focus was measured by using a multichannel spectrometer (B&WTEK, i-trometer) attached at the side port of the microscope. Scanning electron micrographs (SEM) of the surface morphology were taken using a DB-235 system (FEI Company). Sodium azide (Sigma Aldrich) was used to investigate the reaction mechanism related to reactive oxygen species.

Results and discussion

Fluorescence spectral change by laser irradiation

The sample solution (10 μL) was dropped on the oPD film and a green laser beam (2 mW) was focused on the film surface. After the green laser irradiation, a blue laser beam (10 μW) was focused on the same position and the fluorescence spectrum was measured. Figure 3a and 3b show the fluorescence spectra before and after the green laser irradiation for 30 and 60 s in the 100 μM glucose solution and pure water. oPD does not absorb visible light, but polymerized oPDs (poly(oPD)s), including dimers, trimers, oligomers, and polymers, have absorbance in the visible wavelength region because of extension of the π -conjugation length^{21,22}. Therefore, the fluorescence spectra shown in Fig. 3 could be attributed to such polymerized moieties. This measurement was performed at ordinary temperature and pressure; therefore, the oxidative polymerization of a small amount of oPD by oxygen in air was unavoidable. The fluorescence measurement was sufficiently sensitive to detect the fluorescence signal from such polymerized moieties produced by natural oxidation in the oPD film. However, the shape of the fluorescence spectrum depends on the glucose solution and green laser irradiation on the film. The spectral change was not induced when the green laser was focused on the film surface in pure water (Fig. 3a). The spectral peak was located at ~ 560 nm and the spectral shape did not depend on the laser irradiation time. In contrast, a clear spectral

change was found after laser irradiation on the film in glucose solution as shown in Fig. 3b. The spectral broadening in the long-wavelength region indicates the extension of the π -conjugation resulting from further polymerization. Figure 3a and 3b indicate that this film polymerizes more efficiently when the green laser beam is focused in the glucose solution. The mechanism is discussed below.

The oxidization of glucose on the film was catalysed by the GOD included in the film, and then hydrogen peroxide (H_2O_2) was produced. Because H_2O_2 is the substrate of HRP, which was also included in the film, the HRP catalytic reaction occurred successively. oPD is a representative chromogenic species for the HRP reaction, because it forms a dimer (2,3-diaminophenazine: DAP) with orange colour. These reaction mechanisms are schematically described in Figure 1b. Thus, the oxidative polymerization of oPD is catalysed by HRP and H_2O_2 , and the produced dimer absorbs visible light because of extended π -electron conjugation. This reaction is detectable by measuring the optical absorbance of DAP as typically measured in HRP catalytic reactions. In the present experiment, the DAP molecules that formed in the glucose solution absorbed the green laser beam, leading to spectral broadening as shown in Fig. 3b. In Figure 3c, the fluorescence spectra after 60 s irradiation of the laser beam with and without glucose were compared to that of DAP powders. The fluorescence spectrum of DAP was narrower and sharper than that of the oPD film, indicating that the fluorescent molecules included in the oPD film had a longer π -conjugation length than DAP. The

spectral change was not observed at places other than the laser-irradiated spot. Not only the spectral change, but also formation of a small spot was confirmed at the laser-focused point in the glucose solution as shown in the inset of Fig. 3b; this suggests that the morphology change was induced in the laser focus. This small spot was confirmed immediately after 60 s laser irradiation even in pure water, whereas the spectral change was not observed. This morphological change of the film observed using a scanning electron microscope is discussed in the next section. It should be noted that the glucose contributed to the spectral broadening of the fluorescence and the morphological change.

SEM imaging of surface morphology

Figure 4 shows micrographs taken by a scanning electron microscope (SEM) of the sensor surface after green laser irradiation with pure water and 100 μM glucose solution. The green laser beam was focused at 4 points, one by one, for 60 s. The SEM images clearly demonstrated that protrusions formed at the laser focus, where the oxidative polymerization of oPD proceeded. The lateral diameter of protrusions formed without glucose was ~ 800 nm, whereas that of protrusions formed in 100 μM glucose solution was ~ 1800 nm. This is consistent with the finding that poly(oPD) formation is enhanced by glucose and green laser irradiation as discussed above for the fluorescence

experiment. The morphological change was caused by polymerization of oPD, and the degree of the change depended on the glucose concentration. A small deformation formed without glucose (Fig. 4a and 4b) and could have originated from laser absorption by a small amount of poly(oPD) in the film generated by natural oxidation. The formation of large protrusions as shown in in Fig. 4c and 4d was induced by the enhancement of polymerization by cooperation between the enzyme reaction and laser irradiation. Figure 4 indicates that the HRP and GOD enzymes immobilized on a chip by drop-casting maintain their enzymatic activities. A high degree of polymerization increases the free volume, resulting in a protrusion at the laser-irradiated position. It is conceivable that the degree of surface deformation depends on the initial glucose concentration, and the glucose concentration can be estimated by measuring the degree of the morphology change.

Generally the surface deformation and morphological change are evaluated on the nanometre scale by SEM or atomic force microscopy (AFM) measurement; however, these techniques are somewhat time-consuming and laborious. As we demonstrated previously, polymer deposition at the laser focus can be evaluated easily by monitoring the laser intensity reflected from focal spot¹⁶, although oPD and enzymes were in the solution in our previous study.

Glucose detection based on surface deformation

A 10 μL drop of glucose (200, 100, 50, 20 or 10 μM) and ribose (1000 μM , control) solutions was injected in each hole on the sensor chip and a green laser beam (2 mW) was focused on the surface. The temporal change of the reflected laser intensity was measured by a photomultiplier and the output voltage was recorded at a sampling rate of 50 Hz as shown in Fig.5a. The laser irradiation was initiated at 0 s by opening a mechanical shutter. The output at 0 s was attributed to the laser light reflected at the interface between the film and solution. After the laser irradiation, the output intensity was maintained at almost a constant level for some time, and then fluctuations occurred because of the change in surface morphology. A larger fluctuation was observed with a shorter irradiation time in the case of higher glucose concentrations, indicating a morphology change larger and faster than that at a lower glucose concentration. Although similar phenomena were confirmed by focusing laser beams with other wavelengths (473 and 633 nm), the glucose detection with 532 nm laser beam gave the best sensitivity as shown in Figure S2 in supplementary information. The intensity of the laser reflection depends on the changes in size, shape, and refractive index induced by the laser irradiation. Complex variation of the morphology and refractive index results in a complex temporal curve for the laser reflection. This laser reflection corresponds to the backscattering by the produced aggregate. Actually it was theoretically revealed by Mie theory that the backscattering intensity of spherical particles shows a kind of sinusoidal curve as a function of the particle size²³. However, in the present case, the exact solution of the relation of the scattering

intensity vs. the aggregate size cannot be derived from the calculation based on the standard Mie theory, because the shape of the aggregate produced by the laser focus was quite different from the spherical shape as shown in Figure 4. In addition, the size, shape, and refractive index change at every moment during the laser irradiation. The fluctuation of the reflection intensity can be approximately ascribed to the interference of two beams that are reflected at the front and back sides of the aggregate as reported previously¹⁶. However, analysis of the whole shape of the curve is not necessary for glucose sensing. For quantification of the reflection intensity change over a certain time, time-integrated variation $A(t)$ was defined as follows.

$$A(t) = \sum_{t'=0}^t |V(t') - V(0)|$$

The laser irradiation is initiated at $t = 0$ and $V(t)$ is the intensity (output voltage from the photodetector) at t . $V(0)$ is the light intensity at $t = 0$, i.e. the initial intensity of the laser beam reflected at the sensor surface - solution interface. Thus, $A(t)$ indicates the accumulated amount of light intensity change resulting from surface morphology change. When the glucose concentration is high, the morphology change is large and $A(t)$ therefore also has a large value. The accumulation (summation) over t cancels the signal fluctuation. The relationship between $A(t)$ and glucose concentration is shown in Figure 5b, which demonstrates that the glucose concentration can be

evaluated in this manner. This film has a function in which the substrate (glucose) concentration is converted into the light signal of the laser reflection via surface morphology change. Fig. 5b also shows that this film is insensitive to the ribose solution because the GOD reaction is specific to its substrate.

Discussion of the mechanism

The composite film of oPD, GOD and HRP converts enzyme reactions into physical changes in the surface morphology by focusing a green laser beam. The mechanism is tentatively explained as schematically illustrated in Figure 6. As mentioned above, oPD dimer (2,3-diaminophenazine; DAP) molecules are produced by the enzyme reaction (Fig.6-1, 6-2). When a visible laser beam is focused in the oPD solution, including a small amount of DAP, reactive oxygen species (ROS) are produced via laser excitation of DAP (Fig. 6-3), and then further oxidative polymerization of oPD molecules is induced by the ROS (Fig. 6-4 and 6-5). Such polymerized products (dimers, oligomers, and polymers) also absorb the laser beam such that the oxidative polymerization proceeds in a self-catalytic (auto-catalytic) manner in the laser focus (Fig. 6-6). As a result, a nanostructure of polymer aggregates is formed in the laser focus (Fig. 6-7).

Key species in this reaction scheme include ROS such as the superoxide anion, hydroxyl radical and

singlet oxygen produced by the laser excitation of DAP molecules. In particular, singlet oxygen, which has strong oxidation power, is produced by photoexcitation of molecular materials in the presence of oxygen. If the produced ROS is quickly quenched, large morphology changes should be prevented. To confirm this assumption, sodium azide, which is a well-known quencher of singlet oxygen²⁴, was mixed in the solution immediately before laser irradiation. Because the sodium azide may affect the HRP activity²⁵, we waited for 1 minute after the application of glucose, then the addition of sodium azide and the laser irradiation were performed. Figure 7a and 7b show that the change in the reflection intensity of the focused laser beam was suppressed by the addition of sodium azide. We could not find any protrusions caused by the laser irradiation on the film by SEM after the measurement of Figure 7b. This strongly suggests that ROS, particularly the singlet oxygen produced by the laser absorption of DAP, play an important role in nanostructure formation. In this mechanism, DAP absorbs the laser beam and the excited singlet state can decay to lower excited triplet state via intersystem crossing, followed by generation of singlet oxygen. We focused on the similarity of the size of the nanostructure to that of the laser spot as shown in Figure 4, whereas the general photopolymerisation based on the radical polymerisation process has limitations in microfabrication because of the longevity of free radical species and chain reactions²⁶. Oxidative polymerization of oPD was induced by singlet oxygen in this study. Singlet oxygen cannot diffuse beyond the micrometre scale from the laser focus because its longevity in the solution is typically

only a few microseconds²⁷. This short diffusion distance limits nanostructure growth near the laser focus. The singlet oxygen is quenched in a short time but it produced intensely in the laser focus. The nanostructure formation requires effective polymerization in the presence of singlet oxygen at the high density achieved by the focused laser beam.

If the solution does not include DAP, there is no opportunity for changes in surface morphology and the resulting laser reflection to occur. Therefore, the size and deformation speed are strongly dependent on the concentration of dimers included in the solution before laser irradiation and the concentration of dimers included in the original solution can be determined quantitatively by measuring the surface deformation using the reflected intensity of the laser beam.

Conclusions

We succeeded in fabricating enzymatic sensor chips by drop-casting of a solution of oPD, GOD and HRP enzymes. The sensor chip exhibited a characteristic function in which the glucose concentration was converted into a change in the intensity of the focused laser beam via morphological deformation of the sensor surface. The morphological and fluorescence spectral changes induced by the laser irradiation suggested that the polymerization of oPD was enhanced by the focusing of the laser in the presence of glucose. This characteristic reaction required singlet oxygen formation induced by laser irradiation, as supported by testing of the sodium azide effect. Glucose at

concentrations of 10 μM -200 μM was detected with high specificity. Further optimization of the chip preparation and assay conditions could improve the sensitivity, the quantitativity and the dynamic range.

This new methodology is applicable for various assays using HRP reactions and useful for the development of point-of-care testing (POCT) systems. Because the morphology changes ranged in size from sub μm to a few μm as shown in Fig.4, the potential detection volume of the sample could be much smaller than that used in this study (10 μL). This method would be suitable for microanalysis to measure a small-volume sample in a microchamber or microwell, which is an application not suitable for conventional colour detection based on optical absorption. Sensor chip fabrication by the drop-casting method is advantageous for reducing cost, time and labour. In addition, the optical detection system can be constructed without requiring complex optics or costly spectroscopic detectors. The laser focusing and reflection detection employed in this method are already performed by compact and commercially available optical devices, called optical (or laser) pickups, used to read/write optical discs.

Acknowledgements

This work was partially supported by the Nakatani Foundation for Advancement of Measuring Technologies in Biomedical Engineering and the Osaka University LLP (Lean LaunchPad Program)

Gap Fund, which is conducted as a part of the MEXT/JST EDGE program (Enhancing Development of Global Entrepreneur Program).

Notes and references

Department of Applied Physics, Osaka University, 2-1 Yamada-oka, Suita, Osaka 565-0871, Japan.

E-mail: yosikawa@ap.eng.osaka-u.ac.jp

† Electronic supplementary information (ESI) available.

1. M. I. Mohammed and M. P. Y. Desmulliez, *Lab Chip*, 2011, 11, 569-595.
2. S. Kumar, S. Kumar, M. A. Ali, P. Anand, V. V. Agrawal, R. John, S. Maji and B. D. Malhotra, *Biotechnol. J.*, 2013, 8, 1267-1279.
3. J. S. Sun, Y. L. Xianyu and X. Y. Jiang, *Chem. Soc. Rev.*, 2014, 43, 6239-6253.
4. C. L. Wong and M. Olivo, *Plasmonics*, 2014, 9, 809-824.
5. H. M. Hiep, H. Yoshikawa and E. Tamiya, *Anal. Chem.*, 2010, 82, 1221-1227.
6. H. M. Hiep, H. Yoshikawa, M. Saito and E. Tamiya, *Acs Nano*, 2009, 3, 446-452.
7. S. Wu, L. Wang, A. Kroeger, Y. P. Wu, Q. J. Zhang and C. Bubeck, *Soft Matter*, 2011, 7, 11535-11545.
8. Z. Jiang, M. Xu, F. Y. Li and Y. L. Yu, *J. Am. Chem. Soc.*, 2013, 135, 16446-16453.
9. D. Y. Kim, S. K. Tripathy, L. Li and J. Kumar, *Appl. Phys. Lett.*, 1995, 66, 1166-1168.
10. P. Rochon, E. Batalla and A. Natansohn, *Appl. Phys. Lett.*, 1995, 66, 136-138.
11. N. K. Viswanathan, D. Y. Kim, S. P. Bian, J. Williams, W. Liu, L. Li, L. Samuelson, J. Kumar and S. K. Tripathy, *J. Mater. Chem.*, 1999, 9, 1941-1955.
12. C. J. Barrett, A. L. Natansohn and P. L. Rochon, *J. Phys. Chem.*, 1996, 100, 8836-8842.
13. M. Irie, S. Kobatake and M. Horichi, *Science*, 2001, 291, 1769-1772.
14. C. J. Barrett, J. I. Mamiya, K. G. Yager and T. Ikeda, *Soft. Matter.*, 2007, 3, 1249-1261.

15. N. Kurokawa, H. Yoshikawa, H. Masuhara, N. Hirota and K. Hyodo, *J. Phys. Chem. B*, 2002, 106, 10782-10785.
16. H. Yoshikawa, S. Imura and E. Tamiya, *Anal. Chem.*, 2012, 84, 9811-9817.
17. J. F. Liang, Y. T. Li and V. C. Yang, *J. Pharm. Sci.*, 2000, 89, 979-990.
18. B. Wicklein, M. Darder, P. Aranda and E. Ruiz-Hitzky, *Acs Appl. Mater. Inter.*, 2011, 3, 4339-4348.
19. Y. D. Zhang, L. Li, C. H. Yu and T. T. Hei, *Anal. Bioanal. Chem.*, 2011, 401, 2311-2317.
20. V. Sanz, S. de Marcos and J. Galban, *Talanta*, 2009, 78, 846-851.
21. X. G. Li, M. R. Huang, W. Duan and Y. L. Yang, *Chem. Rev.*, 2002, 102, 2925-3030.
22. I. Losito, E. De Giglio, N. Cioffi and C. Malitesta, *J. Mater. Chem.*, 2001, 11, 1812-1817.
23. H. C. v. d. Hulst, *Light Scattering by Small Particles*, Dover Publications, New York, 1981.
24. M. Bancirova, *Luminescence*, 2011, 26, 685-688.
25. T. C. Richardson, D. V. Chapman and E. Heyderman, *J. Clin. Pathol.*, 1983, 36, 411-414.
26. S. Ito, Y. Tanaka, H. Yoshikawa, Y. Ishibashi, H. Miyasaka and H. Masuhara, *J. Am. Chem. Soc.*, 2011, 133, 14472-14475.
27. R. Dedic, A. Molnar, M. Korinek, A. Svoboda, J. Psencik and J. Hala, *J. Lumin.*, 2004, 108, 117-119.

Figure captions

Figure 1

Schematic representations of (a) the fabrication procedure using a drop-casting method and the film structure of the sensor chip. (b) Chromogenic reaction schemes of the glucose detection using oPD.

Figure 2

Experimental setup to induce surface morphology changes and detect the reflected laser intensity.

Figure 3

Fluorescence spectra before (0 s) and after green laser irradiation on the sensor chip for 30 and 60 s in (a) pure water and (b) 100 μM glucose solution. (c) Fluorescence spectra after green laser irradiation for 30 s in pure water (red) and 100 μM glucose solution (blue) compared with the fluorescence spectrum of DAP powder (black). Inset pictures show microscope images at the laser focus before and after 30 s and 60 s laser irradiation.

Figure 4

Micrographs taken by a scanning electron microscope (SEM) of the sensor surface after green laser irradiation with (a and b) pure water and (c and d) 100 μM glucose solution.

Figure 5

(a) Temporal changes of the reflection intensity of the focused green laser beam from sensing spots with 10 μL drops of glucose at 200 (grey), 100 (purple), 50 (green), 20 (blue), and 10 (red) μM and ribose at 1 mM (black) as a negative control solution. (b) Relationship between time-integrated variation of reflection intensity and glucose concentration. Measurements were performed in triplicate. Standard deviations are described as error bars.

Figure 6

Schematic illustration of a tentative reaction mechanism

Figure 7

(a) Temporal changes in the reflection intensity of the focused green laser beam from sensing spots with (a) 10 μL of 200 μM glucose (black) and (b) 10 μL of 200 μM glucose + 10 μL of 100 mM sodium azide (red). The sodium azide solution was added immediately before laser irradiation.

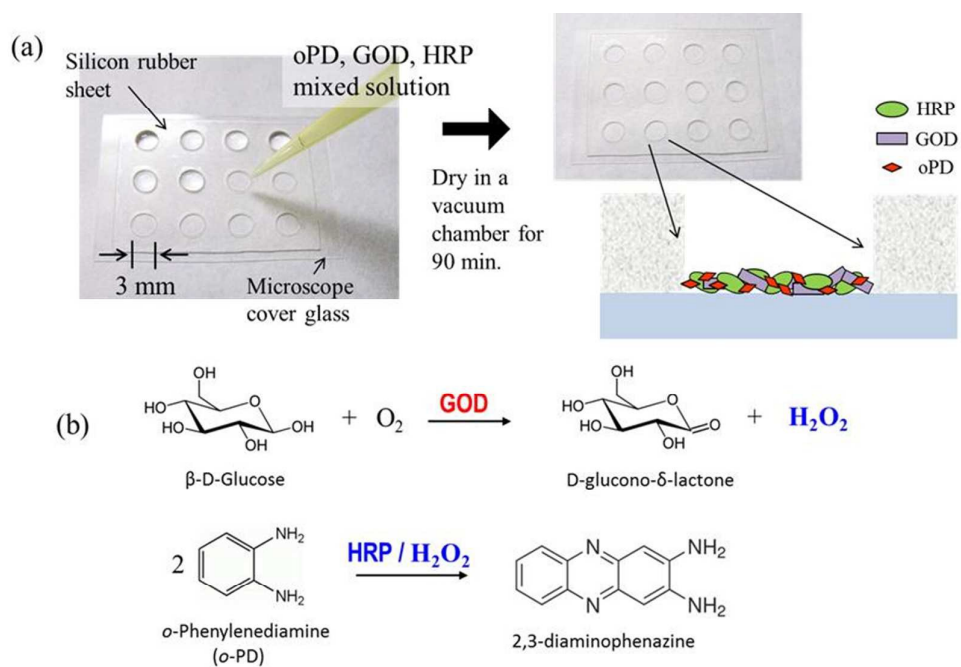


Figure 1

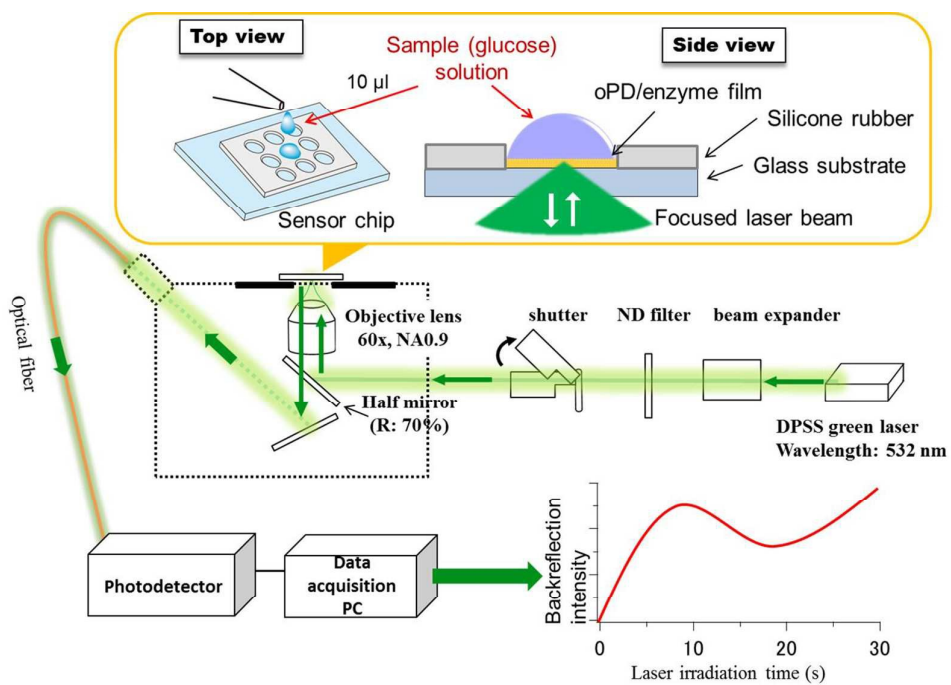


Figure 2

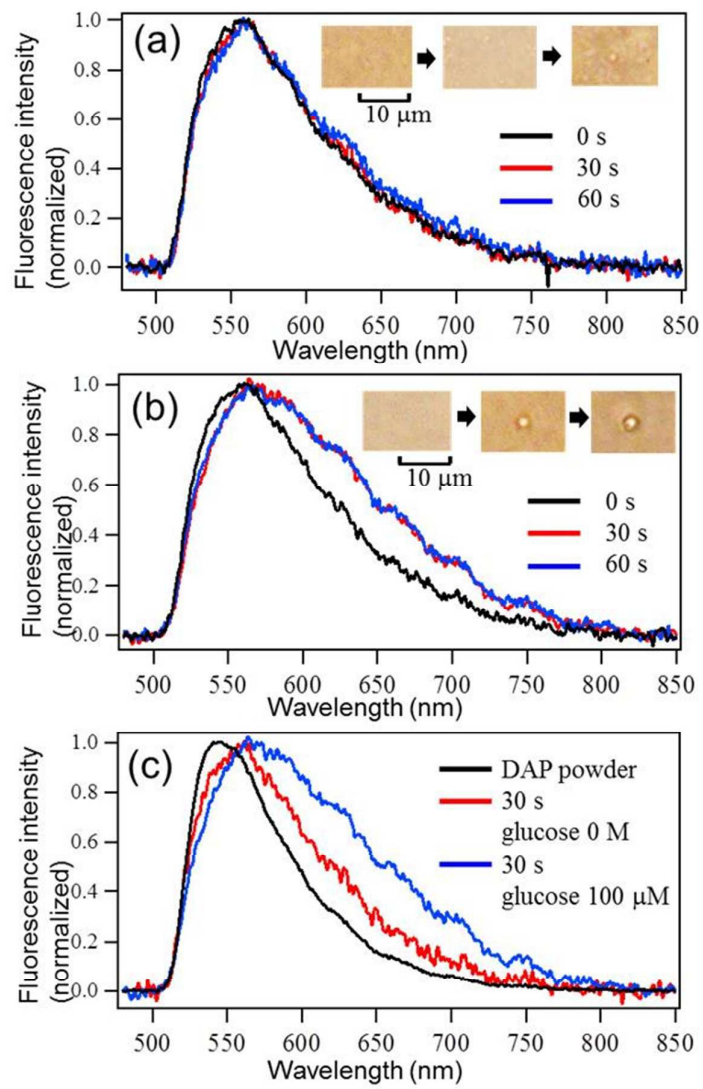


Figure 3

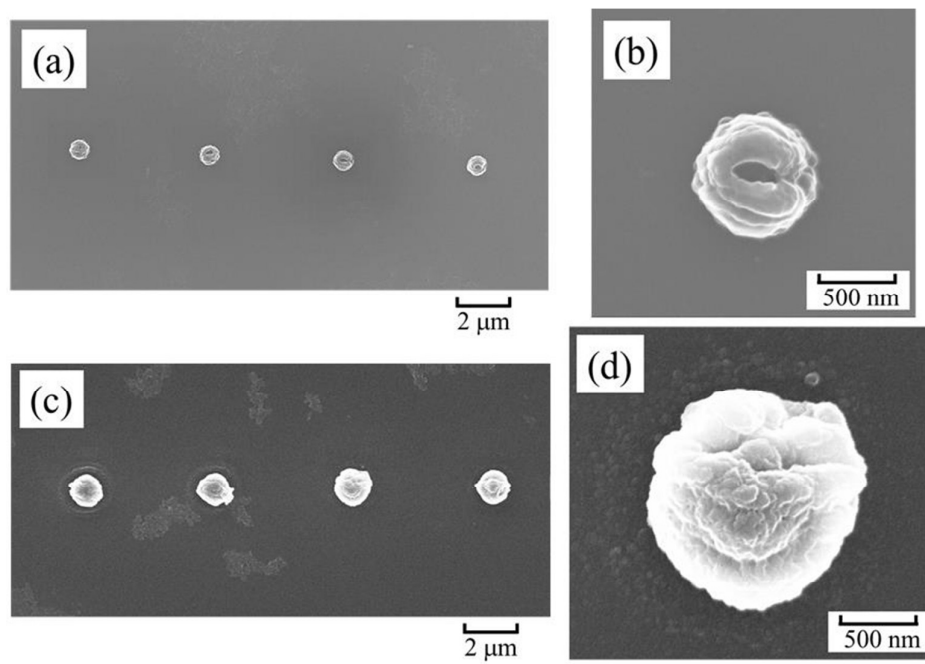


Figure 4

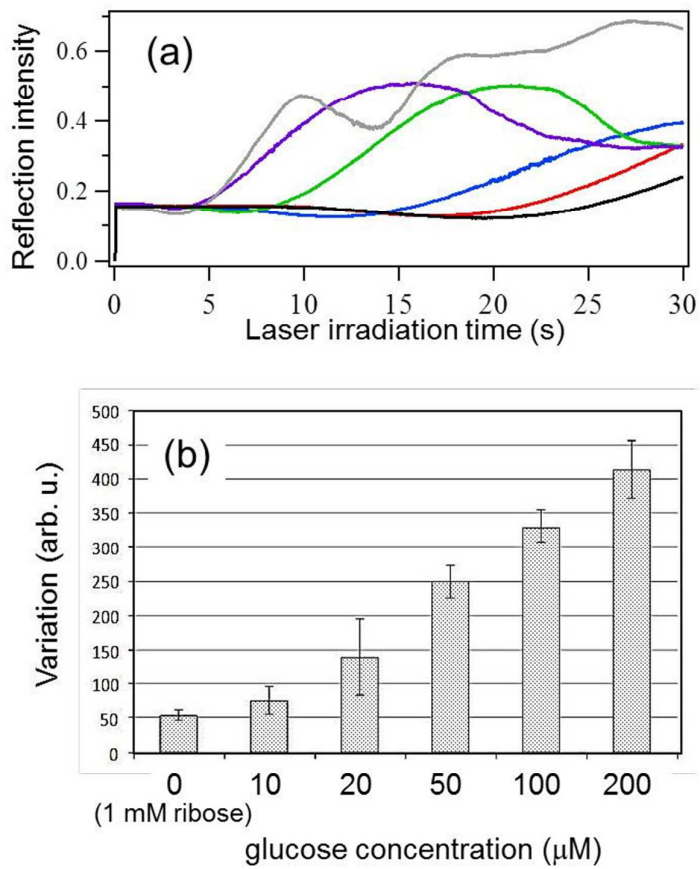


Figure 5

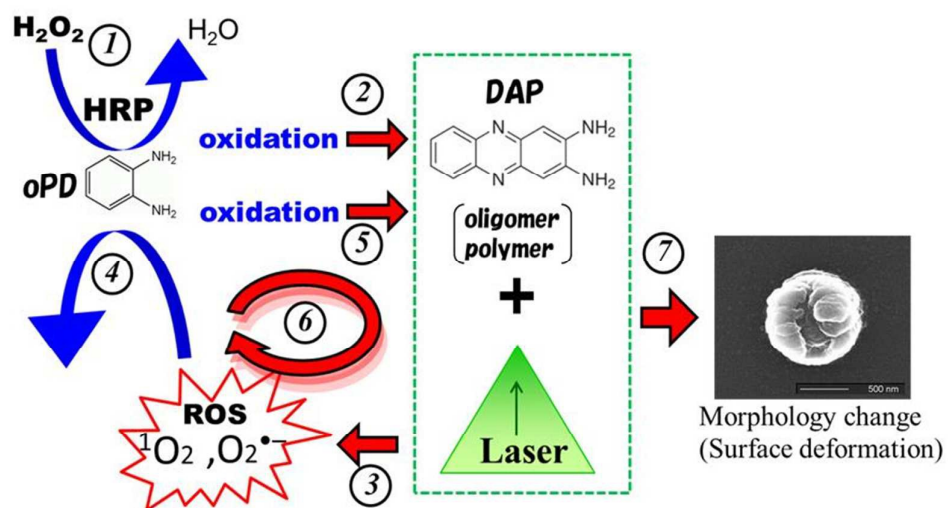


Figure 6

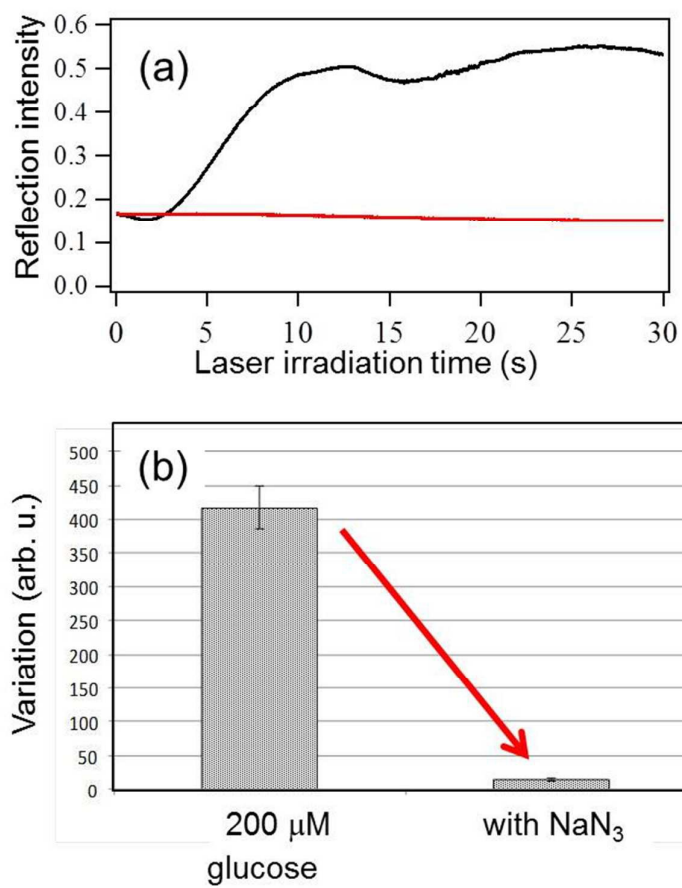


Figure 7